Mechanistic Study of the Addition of Pyrrolidine to α,β-Unsaturated Fischer Carbene Complexes. The Structure of Pentacarbonyl[(2*E*)-3-phenyl-3-*N*-pyrrolidino-1-ethoxypropen-1-ylidene]tungsten(0)

Rolf Pipoh,[1a] Rudi van Eldik,*[,1a] and Gerald Henkel[1b]

Institut für Anorganische Chemie, Universität Witten/Herdecke, Stockumer Strasse 10, 5810 Witten, Germany, and Fachgebiet Anorganische Chemie/Festkörperchemie, Universität Duisburg, 4100 Duisburg 1, Germany

Received October 16, 1992

The addition of pyrrolidine to pentacarbonyl[ethoxy(phenylethynyl)carbene]metal(0) (metal = Cr, Mo, W) gives in good yield yellow compounds which can be characterized as pentacarbonyl-[(2*E*)-3-phenyl-3-*N*-pyrrolidino-1-ethoxypropen-1-ylidene]metal(0). The X-ray structure of the tungsten product was determined. [$C_{20}H_{19}NO_6W$] crystallizes in the triclinic space group $P\bar{1}$ with a = 10.031(3) Å, b = 10.629(3) Å, c = 11.548(3) Å, α = 63.82(2)°, β = 76.57(2)°, γ = 67.99(2)°, and Z = 2. The refinement of the structure converged to R (R_w) = 0.0243 (0.0300) for 4173 observed reflections ($I > 2\sigma(I)$). The temperature, pressure, and solvent dependence of this addition reaction was studied, and the corresponding activation parameters are reported. These data are used to discuss the intimate nature of the addition process in comparison to related data reported for organic reactions in the literature. The data clearly reflect that the investigated reactions proceed via a two step process with a polar transition state for the rate-determining addition step. This is further supported by the absence of a significant deuterium isotope effect.

Introduction

Following the first synthesis of a metal carbene complex by Fischer and Maasböl,[2] these organometallic compounds have become of interest to synthetic organic chemists especially during the last 15 years.[3-6] The α,β-unsaturated carbene complexes exhibit an impressive synthetic potential since they can either react as ester analogues[7-14] due to the isolobal relationship[15] or participate in reactions not related to ester chemistry.[10] These reactions include the well-known Dötz reaction and show a number of advantages such as high regio- and stereoselectivity, large rate enhancement, and easy removal of the pentacarbonylmetal fragment. Although these complexes are of significant interest, the kinetics have rarely been investigated. Besides a kinetic study of a cycloaddition reaction[16] on such α,β-unsaturated complexes, only a few detailed studies for complexes of the type $(CO)_5M(OR^2)$-R^1 (M = Cr, W; R^1 = alkyl, aryl; R^2 = alkyl) exist; these include substitution[17,18] and insertion reactions.[19]

The present investigation was undertaken to study the Michael type addition reaction of secondary amines, in this case pyrrolidine, to α,β-unsaturated complexes (see reaction 1). It was our objective to gain insight into the

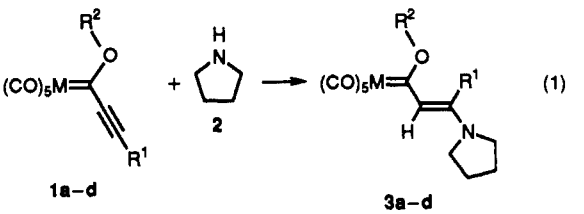

(1)

1a–d 3a–d

1a: M = Cr, R^1 = C_6H_5, R^2 = C_2H_5
1b: M = Mo, R^1 = C_6H_5, R^2 = C_2H_5
1c: M = W, R^1 = C_6H_5, R^2 = C_2H_5
1d: M = W, R^1 = CH_3, R^2 = CH_3

intimate nature of the addition mechanism since these β-aminovinyl-substituted carbene complexes, which are well documented in the literature,[20-27] are often used as

(1) (a) Universität Witten/Herdecke. (b) Universität Duisburg.
(2) Fischer, E. O.; Maasböl, A. *Angew. Chem., Int. Ed. Engl.* **1964**, *3*, 580.
(3) Dötz, K. H.; Fischer, H.; Hofmann, P.; Kreissl, F. R.; Schubert, U.; Weiss, K. *Transition Metal Carbene Complexes*; Verlag Chemie: Weinheim, Germany, 1983.
(4) Dötz, K. H. *Angew. Chem., Int. Ed. Engl.* **1984**, *23*, 587.
(5) Wulff, W. D.; Tang, P. C.; Chan, K. S.; McCallum, J. S.; Yang, D. C.; Gilbertson, S. R. *Tetrahedron* **1985**, *41*, 5813.
(6) Brookhart, M.; Studabaker, W. B. *Chem. Rev.* **1987**, *87*, 411.
(7) Wulff, W. D.; Yang, D. C.; Murray, C. K. *Pure Appl. Chem.* **1988**, *60*, 137.
(8) Wulff, W. D.; Yang, D. C. *J. Am. Chem. Soc.* **1983**, *105*, 6726.
(9) Wulff, W. D.; Yang, D. C. *J. Am. Chem. Soc.* **1984**, *106*, 7565.
(10) Dötz, K. H. *New J. Chem.* **1990**, *14*, 433.
(11) Dötz, K. H.; Kuhn, W.; Müller, G.; Huber, B.; Alt, H. G. *Angew. Chem.* **1986**, *98*, 826.
(12) Dötz, K. H.; Kuhn, W. *J. Organomet. Chem.* **1985**, *286*, C23.
(13) Faron, K. L.; Wulff, W. D. *J. Am. Chem. Soc.* **1988**, *110*, 8727.
(14) Wulff, W. D.; Bauta, W. E.; Kaesler, R. W.; Lankford, P. J.; Miller, R. A.; Murray, C. K.; Yang, D. C. *J. Am. Chem. Soc.* **1990**, *112*, 3642.
(15) Hoffmann, R. *Angew. Chem.* **1982**, *94*, 725.
(16) Pipoh, R.; van Eldik, R.; Wang, S. L. B.; Wulff, W. D. *Organometallics* **1992**, *11*, 490.
(17) Werner, H.; Fischer, E. O.; Heckl, B.; Kreiter, C. G. *J. Organomet. Chem.* **1971**, *28*, 367.
(18) Heckl, B.; Werner, H.; Fischer, E. O. *Angew. Chem.* **1968**, *80*, 847.
(19) Schneider, K. J.; Neubrand, A.; van Eldik, R.; Fischer, H. *Organometallics* **1992**, *11*, 267.
(20) Deutsch, M.; Lackmann, R.; Stein, F.; de Meijere, A. *Synlett* **1991**, 324.
(21) Fischer, E. O.; Kreissl, F. R. *J. Organomet. Chem.* **1972**, *35*, C47.
(22) Fischer, E. O.; Kalder, H. J. *J. Organomet. Chem.* **1977**, *131*, 57.
(23) Aumann, R.; Hinterding, P. *Chem. Ber.* **1990**, *123*, 611.
(24) Aumann, R.; Hinterding, P.; Krüger, C.; Betz, P. *Chem. Ber.* **1990**, *123*, 1847.
(25) Aumann, R.; Hinterding, P. *Chem. Ber.* **1990**, *123*, 2047.

0276-7333/93/2312-2236$04.00/0

intermediates in synthetic routes to organic materials. By way of comparison, a typical substitution reaction of the type shown in (2) was also investigated. The spectroscopic

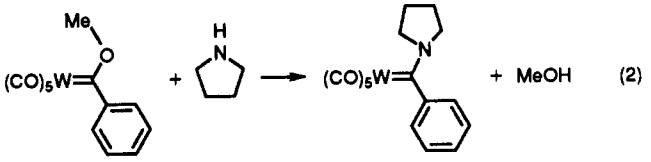

4 5

and kinetic information on reactions 1 and 2 differ significantly and enable a clear differentiation between these processes.

Experimental Section

Materials. All experiments were carried out under an atmosphere of argon. Glassware was soaked in KOH-saturated 2-propanol, rinsed thoroughly with distilled water, and oven dried at 100 °C. The carbene complexes 1a–d[12,21,28] and 4[29] were prepared by literature procedures. Pyrrolidine (Merck) was distilled under argon and stored over molecular sieves (Roth, 3 Å) in the dark. Solvents were dried by standard methods (CaH_2 or molecular sieves) and then distilled prior to use.

General Procedure for the Isolation of the Carbene Complexes 3a, 3c, 3d, and 5 in Reactions 1 and 2. The reactions were performed in a flask containing a stirring bar. The carbene complex was dissolved in acetonitrile and then mixed with an excess of pyrrolidine. During the mixing the color changed spontaneously from deep red to yellow. The solvent and excess of pyrrolidine were removed under reduced pressure, and the crude product was purified by column chromatography on silica gel with pentane/benzene (2:1). The yellow fraction was collected and the eluent evaporated under vacuum. The infrared spectra were collected on a Nicolet FT-IR SX, the NMR spectra on a Bruker AM 400 WB with $CDCl_3$ as internal reference, and the mass spectra, on a Varian MAT 311A. Elemental analyses were carried out by Mikroanalytisches Laboratorium Beller, Göttingen, Germany.

Pentacarbonyl[(2*E*)-3-phenyl-3-*N*-pyrrolidino-1-ethoxypropen-1-ylidene]chromium(0), 3a, Spectral Data. ^{1}H-NMR, δ: 0.55 (t, 3H), 1.83 (m, 2H), 2.05 (m, 2H), 3.05 (m, 2H), 3.59 (m, 2H), 4.15 (q, 2H), 6.44 (s, 1H), 7.14–7.36 (m, 5H). IR (hexane, cm^{-1}): 1926 (vs), 1945 (s), 1984 (w), 2045 (m). Anal. Calcd (Found): C, 57.0 (57.3); H, 4.51 (4.46); N, 3.33 (3.37).

Pentacarbonyl[(2*E*)-3-phenyl-3-*N*-pyrrolidino-1-ethoxypropen-1-ylidene]tungsten(0), 3c, Spectral Data. ^{1}H-NMR, δ: 0.57 (t, 3H), 1.87 (m, 2H), 2.07 (m, 2H), 3.06 (m, 2H), 3.71 (m, 2H), 4.07 (q, 2H), 6.48 (s, 1H), 7.13–7.43 (m, 5H). ^{13}C-NMR, δ: 14.0 (OCH_2CH_3); 27.3, 49.3, 51.2 (NC_4H_8); 75.3 (O–CH_2); 121.3, 126.7, 128, 129.2 (C_6H_5); 138.3 (C(2)); 155.3 (C(3)); 200.5 (*cis*-CO); 204.7 (*trans*-CO); 270.5 (C(1)). IR (hexane, cm^{-1}): 1924 (vs), 1959 (w), 2054 (m). Anal. Calcd (Found): C, 43.7 (43.7); H, 3.44 (3.15); N, 2.53 (2.61). Mass spectra, m/e: 547, 549, 551 (M^+).

Pentacarbonyl[(2*E*)-3-methyl-3-*N*-pyrrolidino-1-methoxypropen-1-ylidene]tungsten(0), 3d, Spectral Data. ^{1}H-NMR, δ: 2.02 (m, 4H), 2.36 (s, 3H), 3.50 (m, 4H), 4.23 (s, 3H), 6.37 (s, 1H). ^{13}C-NMR δ: 26.8, 49.3, 52.1 (NC_4H_8); 68.7 (O–CH_3); 121.8 (C(2)); 158.3 (C(3)); 199.4 (*cis*-CO); 203.5 (*trans*-CO); 268.8 (C(1)). IR (hexane, cm^{-1}): 1922 (vs), 1961 (vw), 2056 (m). Anal. Calcd (Found): C, 35.2 (35.5); H, 3.15 (2.98); N, 2.94 (3.10).

Pentacarbonyl[phenyl-*N*-pyrrolidinocarbene]tungsten(0), 5, Spectral Data. ^{1}H-NMR, δ: 2.23 (m, 2H), 2.39 (m, 2H), 3.43 (m, 2H), 4.36 (m, 2H), 6.95 (m, 1H), 7.30 (m, 2H), 7.54 (m, 2H). IR (hexane, cm^{-1}): 1922 (vs), 1959 (sh), 2054 (m). Anal. Calcd (Found): C, 39.76 (40.10); H, 2.69 (2.38); N, 2.90 (2.85).

Table I. Details of Data Collection and Structure Refinement for $[C_{20}H_{19}NO_6W]$

formula	$C_{20}H_{19}NO_6W$
fw	553.21
cryst size, mm	ca. 0.33 × 0.23 × 0.21
temp, K	150
cryst syst	triclinic
space group	*P*1
a, Å	10.031(3)
b, Å	10.629(3)
c, Å	11.548(3)
α, deg	63.82(2)
β, deg	76.57(2)
γ, deg	67.99(2)
V, Å^3	1021
Z	2
μ(Mo Kα), mm^{-1}	5.69
D_x, g cm^{-3}	1.799
measuring device	Siemens P4RA four-circle diffractometer (rotating anode, gaphite monochromator, scintillation counter, λ = 0.710 73 Å (Mo Kα))
scan mode	ω-scan
abs corr	empirical (ψ-scan)
transm range	0.452–0.253
scan range, deg	$4 < 2\theta < 54$ ($+h,\pm k,\pm l$)
scan speed	intensity dependent (4–29° min^{-1})
structure soln	SHELXTL PLUS (direct methods)
refinement	full-matrix least squares, non-hydrogen atoms anisotropic, H atoms fixed at idealized positions, one scaling factor, one isotropic extinction parameter
weighting scheme	$w = [\sigma^2(F_o) + (0.01F_o)^2]^{-1}$
no. of ind reflns	4458, of which 4173 are observed ($I > 2\sigma(I)$)
no. of variables	259
$R = (\sum\|\|F_o\| - \|F_c\|\|)/\sum\|F_o\|$	0.0243
$R_w = [\sum w(\|F_o\| - \|F_c\|)^2/\sum wF_o^2]^{1/2}$	0.0300

Synthesis of *N*-Deuteriopyrrolidine. In a flask containing a stirring bar and equipped with a condenser, 10 mL of pyrrolidine was mixed with 10 mL of deuterium oxide and the mixture was refluxed for 48 h. The solution was then saturated with NaCl and the deuterated amine extracted by ether. The ether was evaporated and the crude *N*-deuteriopyrrolidine distilled (bp 90–91 °C). The extent of deuteration was checked by NMR spectroscopy.

X-ray Structure Determination of 3c. A yellow crystal was mounted at the top of a glass capillary and cooled down to approximately 150 K under a stream of cold nitrogen gas by using a Siemens LT-2 cooling device. The orientation matrix and the unit cell dimensions were obtained by a least-squares fit of the setting angles of 18 high-angle reflections. X-ray intensities were collected with a Siemens P4RA four-circle diffractometer equipped with a Mo Kα source (rotating anode generator), a scintillation counter, and a graphite monochromator. Data reduction was done by applying Lorentz and polarization corrections.

All calculations were done by using the programs of the SHELXTL PLUS program package.[30] Atomic scattering factors for spherical neutral free atoms (bonded for hydrogen) were taken from standard sources,[31] and anomalous dispersion was taken into account for the non-hydrogen atoms. Details of the crystal structure analysis, including the final least-squares refinement, are provided in Table I. Positional parameters are given in Table II, and bond distances and valence angles are provided in Table III.

(26) Lattuda, L.; Licandro, E.; Papagni, A.; Maiorana, S.; Villa, A. C.; Guastini, C. *J. Chem. Soc., Chem. Commun.* **1988**, 1092.
(27) de Meijere, A.; Kaufmann, A.; Lackmann, R.; Militzer, H. C.; Reiser, O.; Schömenauer, S.; Weier, A. *Organometallics in Organic Synthesis II*; Springer Verlag: Germany, 1989.
(28) Chan, K. S.; Wulff, W. D. *J. Am. Chem. Soc.* **1986**, *108*, 5229.
(29) Fischer, E. O.; Heckl, B.; Dötz, K. H.; Müller, J.; Werner, H. *J. Organomet. Chem.* **1969**, *16*, P29.
(30) SHELXTL PLUS program package, Siemens Analytical X-ray Instruments Inc., Madison, WI.
(31) Kynoch, R. *International Tables for X-Ray Crystallography*; Kynoch Press: Birmingham, U.K., 1974.

Table II. Coordinates and Coefficients of the Equivalent Isotropic Temperature Factors (without H Atoms)[a] for $[C_{20}H_{19}NO_6W]$

atom	x	y	z	U
W	0.28463(2)	0.32633(2)	0.53516(1)	0.02188(7)
O(1)	0.1735(4)	0.6678(3)	0.4873(3)	0.036(1)
O(2)	0.0128(4)	0.2622(4)	0.7275(3)	0.046(2)
O(3)	0.1235(4)	0.4176(4)	0.2918(3)	0.045(2)
O(4)	0.3517(4)	-0.0012(3)	0.5617(3)	0.038(1)
O(5)	0.5738(3)	0.3583(4)	0.3546(3)	0.041(2)
O(6)	0.3798(3)	0.2853(3)	0.8040(3)	0.027(1)
N	0.7916(3)	0.0077(3)	0.7787(3)	0.027(1)
C(1)	0.2161(4)	0.5444(4)	0.5089(4)	0.027(2)
C(2)	0.1094(4)	0.2898(4)	0.6585(4)	0.030(2)
C(3)	0.1811(5)	0.3867(4)	0.3805(4)	0.032(2)
C(4)	0.3337(4)	0.1142(4)	0.5540(4)	0.027(2)
C(5)	0.4706(5)	0.3483(4)	0.4187(4)	0.031(2)
C(6)	0.4186(4)	0.2513(4)	0.6989(3)	0.021(1)
C(7)	0.2418(5)	0.3862(5)	0.8221(4)	0.036(2)
C(8)	0.2407(5)	0.4022(6)	0.9450(5)	0.042(2)
C(9)	0.5603(4)	0.1544(4)	0.7016(3)	0.023(1)
C(10)	0.6647(4)	0.1069(4)	0.7865(3)	0.023(1)
C(11)	0.6464(4)	0.1665(4)	0.8870(3)	0.023(1)
C(12)	0.6154(5)	0.0859(5)	1.0167(4)	0.031(2)
C(13)	0.5992(5)	0.1451(5)	1.1066(4)	0.038(2)
C(14)	0.6141(5)	0.2809(5)	1.0700(4)	0.038(2)
C(15)	0.6489(5)	0.3604(5)	0.9401(4)	0.034(2)
C(16)	0.6636(4)	0.3035(4)	0.8489(4)	0.028(2)
C(17)	0.9144(5)	-0.0415(5)	0.8554(5)	0.038(2)
C(18)	1.0417(6)	-0.1034(9)	0.7749(8)	0.084(5)
C(19)	0.9859(6)	-0.1650(7)	0.7125(7)	0.065(3)
C(20)	0.8323(5)	-0.0602(5)	0.6837(5)	0.039(2)

[a] The equivalent isotropic temperature factor is defined as one-third of the trace of the orthogonalized U_{ij} tensor.

Kinetic Measurements. The overall addition reaction could be studied using a rapid-scan spectrophotometer system consisting of a Durrum D110 stopped-flow unit and an OSMA detector (Spectroscopy Instruments, Garching, FRG). The progress of reaction 1 was followed by the disappearance of the MLCT band at 489 nm for 1a, 483 nm for 1b, 475 nm for 1c (in this case also the appearance of the product MLCT band at 420 nm was observed), and 427 nm for 1d. For reaction 2 the decrease of the MLCT band at 400 nm was monitored. Ambient pressure kinetic measurements were performed on a Durrum D110 stopped-flow instrument, whereas at elevated pressure on a homemade high pressure stopped-flow unit.[32] Both instruments were thermostated to ±0.1 °C. Data acquisition and handling were performed on an on-line computer system.[33] The corresponding pseudo-first-order plots were linear over the studied time range and the estimated rate constants (average of at least five kinetic runs) were reproducible to within 5%. Typical experimental conditions were [complex] = (1–3) × 10^{-5} M and [pyrrolidine] = (3–30) × 10^{-4} M.

Results and Discussion

Identification of Products. The products formed in the addition of pyrrolidine to various carbene complexes (see reaction 1) and in the substitution reaction (2) were isolated, fully characterized, and shown to be similar to those obtained in previous studies.[20-22,34,35]

The products are yellow solids that exhibit two significant carbonyl bands at ca. 1924 and ca. 2045 (M = Cr) or 2055 cm^{-1} (M = W) for reactions 1 and 2, respectively. In all cases the addition products 3a–d are isomers which were assigned as *E* on the basis of the chemical shift by ^{1}H-NMR and ^{13}C-NMR by comparison to similar complexes and ultimately by X-ray diffraction analysis of 3c. The observed four signals in the ^{1}H-NMR for the pyrrolidino ligand in the case of 3a and 3c can be explained in terms of the considerable double bond character of the C–N bond which handicaps the free rotation of the pyrrolidine ligand (see structural data for 3c). The ^{1}H signals show an upfield shift due to the anisotropic effect of the phenyl ring. This effect is not present in the case of the methoxy complex (3d), where only two ^{1}H signals are observed for the NC_4H_8 ligand.

Table III. Distances (Å) and Angles (deg) for $[C_{20}H_{19}NO_6W]$

W–C(1)	2.054(5)	C(1)–W–C(2)	92.0(2)
W–C(2)	2.032(4)	C(1)–W–C(3)	88.3(2)
W–C(3)	2.007(5)	C(1)–W–C(4)	174.2(2)
W–C(4)	2.038(5)	C(1)–W–C(5)	91.3(2)
W–C(5)	2.056(4)	C(1)–W–C(6)	94.1(2)
W–C(6)	2.250(4)	C(2)–W–C(3)	92.0(2)
		C(2)–W–C(4)	85.1(2)
		C(2)–W–C(5)	175.9(1)
		C(2)–W–C(6)	92.3(2)
		C(3)–W–C(4)	86.8(2)
		C(3)–W–C(5)	90.6(2)
		C(3)–W–C(6)	175.0(1)
		C(4)–W–C(5)	91.8(2)
		C(4)–W–C(6)	91.0(2)
		C(5)–W–C(6)	85.0(2)
C(1)–O(1)	1.143(5)	W–C(1)–O(1)	175.4(4)
C(2)–O(2)	1.144(5)	W–C(2)–O(2)	176.4(4)
C(3)–O(3)	1.152(7)	W–C(3)–O(3)	178.2(4)
C(4)–O(4)	1.137(6)	W–C(4)–O(4)	175.1(4)
C(5)–O(5)	1.135(5)	W–C(5)–O(5)	178.9(4)
C(6)–O(6)	1.348(5)	W–C(6)–O(6)	127.9(2)
C(6)–C(9)	1.407(5)	W–C(6)–C(9)	120.6(3)
		O(6)–C(6)–C(9)	111.5(4)
O(6)–C(7)	1.435(5)	C(6)–O(6)–C(7)	122.3(3)
C(7)–C(8)	1.500(9)	O(6)–C(7)–C(8)	107.1(4)
C(9)–C(10)	1.400(6)	C(6)–C(9)–C(10)	129.2(4)
C(10)–C(11)	1.497(7)	N–C(10)–C(9)	120.8(4)
		N–C(10)–C(11)	115.3(4)
		C(9)–C(10)–C(11)	123.8(3)
C(11)–C(12)	1.387(5)	C(10)–C(11)–C(12)	121.0(4)
		C(10)–C(11)–C(16)	119.0(3)
		C(12)–C(11)–C(16)	120.0(5)
C(12)–C(13)	1.386(8)	C(11)–C(12)–C(13)	119.2(5)
C(13)–C(14)	1.371(8)	C(12)–C(13)–C(14)	121.3(4)
C(14)–C(15)	1.395(6)	C(13)–C(14)–C(15)	119.6(5)
C(15)–C(16)	1.385(8)	C(14)–C(15)–C(16)	119.7(5)
C(11)–C(16)	1.390(7)	C(11)–C(16)–C(15)	120.2(3)
N–C(10)	1.328(4)	C(10)–N–C(17)	125.7(4)
N–C(17)	1.480(7)	C(10)–N–C(20)	123.6(4)
		C(17)–N–C(20)	110.5(3)
C(17)–C(18)	1.511(9)	N–C(17)–C(18)	102.8(5)
C(18)–C(19)	1.463(15)	C(17)–C(18)–C(19)	105.6(6)
C(19)–C(20)	1.533(7)	C(18)–C(19)–C(20)	104.4(6)
C(20)–N	1.469(8)	N–C(20)–C(19)	104.2(5)

Crystal Structure of 3c. From the literature it is known that octahedral transition metal carbene complexes show a number of common structural features concerning the carbene ligand.[3] This enables us to compare the X-ray structure analysis of 3c (Figure 1) to related chromium carbene complexes, since much more X-ray data are available for first row transition metal compounds than for analogous complexes of the heavier metals.

The atoms O(6), C(6), C(9), C(10), and N of the ligand and the metal center define a common plane (mean deviation 0.033 Å). The W–C(6) carbene distance [2.250(4) Å] is in the upper range of values generally observed. A similar picture was obtained for a related β-aminovinyl-substituted chromium carbene complex,[26] where the Cr–C (carbene) distance [2.130(5) Å] is also in the upper range of normally observed values.

(32) van Eldik, R.; Palmer, D. A.; Schmidt, R.; Kelm, H. *Inorg. Chim. Acta* **1981**, *50*, 131.
(33) Kraft, J.; Wieland, S.; Kraft, U.; van Eldik, R. *GIT Fachz. Lab.* **1987**, *31*, 560.
(34) Köhler, F. H.; Kalder, H. J.; Fischer, E. O. *J. Organomet. Chem.* **1976**, *113*, 11.
(35) Fischer, E. O.; Leupold, M. *Chem. Ber.* **1972**, *105*, 599.

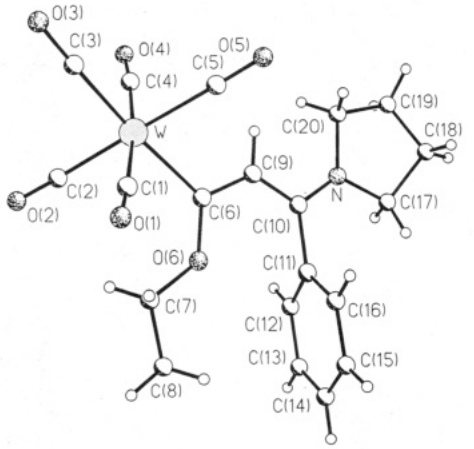

Figure 1. Crystal structure of **3c**.

The bond distances C(6)–C(9) [1.407(5) Å], C(9)–C(10) [1.400(6) Å], and C(10)–N [1.328(4) Å] are indicative for a π-delocalization within the carbene ligand with a significant double bond character between the carbon and the nitrogen atom. A C–N bond of comparable length was also found in the above mentioned chromium β-aminovinyl complex [1.315(6) Å]. Further strong support for such a double bond character was obtained from a structure of a β-imminium ion containing chromium carbene complex,[24] where a C–N distance of 1.277(4) Å was measured. The C–O distance in the carbene ligand is much more appropriate for a single bond.

Kinetic Investigations. Reaction 1 is accompanied by characteristic changes of the MLCT (π–π^*)[36] bands, as indicated in Figure 2a,b, which allow kinetic measurements at either the absorbance increase or absorbance decrease. A series of experiments for the carbene complex 1c clearly indicated that similar rate constants are obtained at λ = 420 nm (increase in absorbance) and λ = 475 nm (decrease in absorbance) (see Figure 3). The kinetic measurements were therefore performed at 475 nm (decrease in absorbance). In all cases the observed pseudo-first-order rate constants varied linearly with the pyrrolidine concentration. Plots of k_{obs} versus [pyrrolidine] exhibited no meaningful intercepts, as shown in Figure 3 for 1c, which can be expressed as in eq 3. The absence of a significant

$$k_{obs} = k[\text{pyrrolidine}] \qquad (3)$$

intercept indicates that, under the selected conditions, no parallel pyrrolidine concentration independent reaction occurs. The absence of an intercept also indicates that the addition reactions go to completion, which is in agreement with the spectroscopic observations.

Reaction 2 is also accompanied by characteristic changes of the MLCT (π–π^*)[35,37] band (see Figure 2c), and the measurements were performed at 400 nm. For reaction 2 the observed pseudo-first-order rate constant varied nonlinearly with the pyrrolidine concentration, as shown in Figure 4. The corresponding reaction order was determined from a plot of log k_{obs} versus log [pyrrolidine] (slope = 2). The plot of k_{obs} versus [pyrrolidine]^2 leads to a straight line with no meaningful intercept, so that the rate law can be expressed as in (4). This rate law is in good agreement with two earlier studies where the aminolysis of $(CO)_5MC(OR^2)(R^1)$ was investigated,[17,18] and

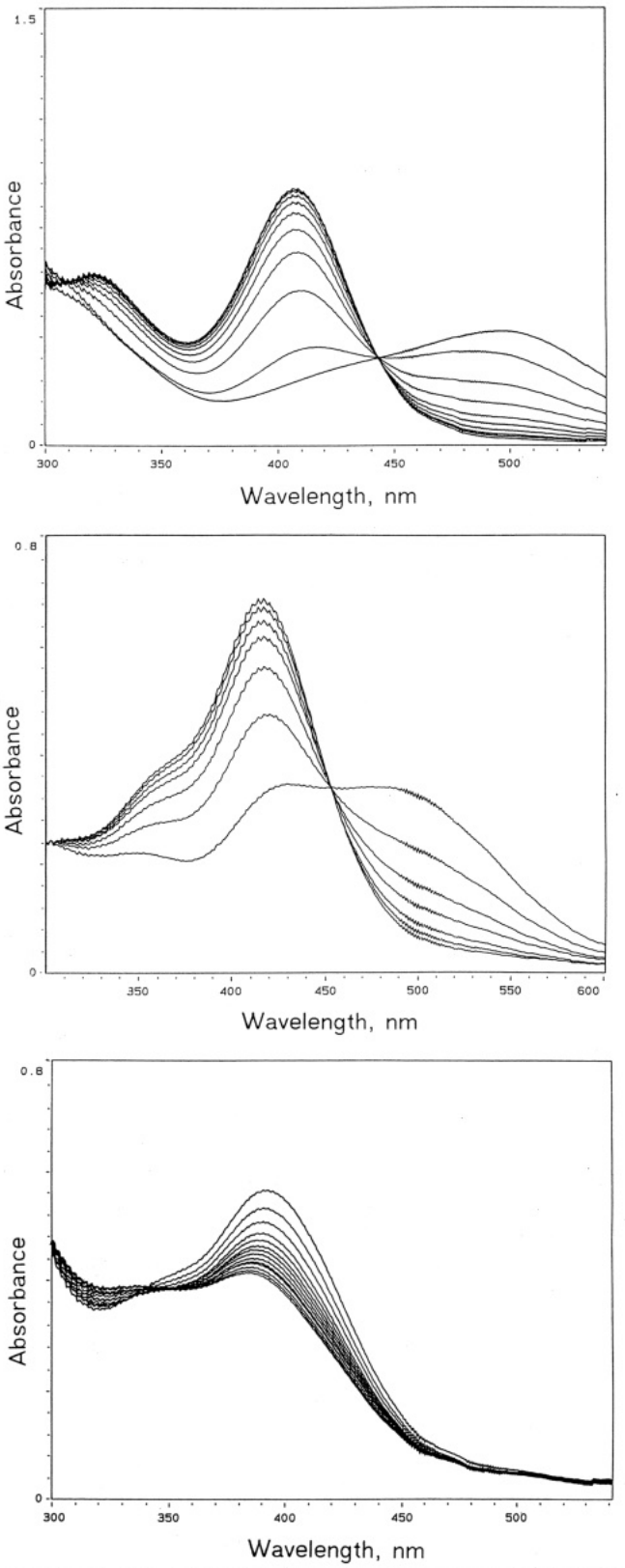

Figure 2. Repetitive scan spectra recorded for reactions 1 and 2 in acetonitrile at 25 °C. Experimental conditions: [complex] = (1–3) × 10^{-5} M; [pyrrolidine] = (3–10) × 10^{-4} M; Δt = 33 ms. Key: (a, top) reaction 1, 1a; (b, middle) reaction 1, 1c; (c, bottom) reaction 2.

where different reaction orders (higher than 1) were obtained depending on the nature of the solvent. A further indication that the process is not bimolecular was obtained from the rapid-scan measurements (see Figure 2c). The spectra exhibit no clean isosbestic point in comparison to Figure 2a,b. These observations are in line with the earlier

(36) Fischer, E. O.; Kreiter, C. G.; Kollmeier, H. J.; Müller, J.; Fischer, R. D. *J. Organomet. Chem.* **1971**, *28*, 237.
(37) Fischer, E. O.; Heckl, B. *J. Organomet. Chem.* **1971**, *28*, 359.

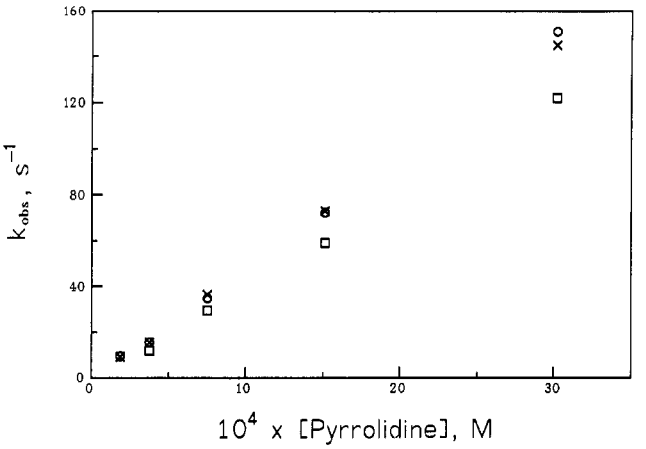

Figure 3. Plot of k_{obs} versus [pyrrolidine] for reaction 1 in acetonitrile at 25 °C, [1c] = 3×10^{-5} M. Key: (○) increase in absorbance of 3c at 420 nm, pyrrolidine; (×) decrease in absorbance of 1c at 475 nm, pyrrolidine; (□) decrease in absorbance of 1c at 475 nm, *N*-deuteriopyrrolidine.

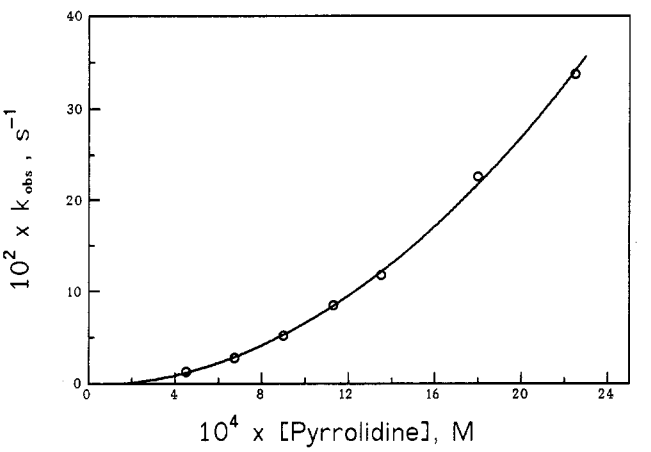

Figure 4. Plot of k_{obs} versus [pyrrolidine] for reaction 2 in acetonitrile at 25 °C, [1c] = 3×10^{-5} M.

$$k_{obs} = kK[\text{pyrrolidine}]^2 \quad (4)$$

proposed mechanism[17,18] where in the first step (for which the equilibrium constant is K) the amine attacks the alkoxy oxygen and weakens the partial double bond between the carbon (carbene) and the oxygen atoms. The second step (for which the rate constant is k) was assigned to the nucleophilic attack of a second amine molecule on the carbon (carbene) which leads to the final substitution product.

For reaction 1 the values of the second-order rate constant k are summarized as a function of temperature and pressure for the different carbene complexes in Table IV, and the corresponding activation parameters are reported in Table V. Plots on ln k_{obs} versus pressure were linear within the experimental error limits over the investigated pressure range, and $\Delta V^{\ddagger}$ values were calculated from the slope ($= -\Delta V^{\ddagger}/RT$) of such plots in the usual way. The data in Table IV clearly demonstrate that the reactivity of the carbene complexes *1*a–c increases in the order Mo > W > Cr for reaction 1. This effect of the metal on the reactivity is also known and described for substitution reactions of metal carbonyl complexes of group VIb.[38] Table IV further indicates that the tungsten complex 1c reacts faster than the corresponding chromium complex 1a, a result which was also found in the [2 + 2] cycloaddition study[16] on such α,β-acetylene carbene complexes. Table IV also demonstrates that the reaction is much more affected by moderate pressures than by increasing the temperature. This effect is independent of the nature of the solvent (see Table VI) and rather unusual in comparison to other documented results.[16,19]

(38) Graham, J. R.; Angelici, R. J. *Inorg. Chem.* **1967**, *6*, 2082.

Table IV. Rate Constants as a Function of Temperature and Pressure for the Addition of Pyrrolidine to Different α,β-Unsaturated Fischer Carbene Complexes in Acetonitrile

complex	temp, °C	pressure, MPa	$10^{-4}k$, M^{-1} s^{-1}
1a	15.0	0.1	2.73 ± 0.05
	20.0		2.82 ± 0.02
	25.0		2.92 ± 0.04
	30.0		3.02 ± 0.02
	35.0		3.08 ± 0.03
	25.0	10	2.38 ± 0.07
		50	3.21 ± 0.14
		100	4.35 ± 0.16
		150	6.13 ± 0.07
1b	15.1	0.1	9.4 ± 0.3
	25.0		10.3 ± 0.5
	35.0		11.3 ± 0.4
	25.0	10	7.6 ± 0.7
		50	10.1 ± 0.2
		100	14.0 ± 0.2
		150	19.2 ● 0.3
1c	15.2	0.1	4.26 ● 0.09
	20.4		4.66 ± 0.09
	25.2		5.01 ● 0.05
	30.0		5.46 ± 0.09
	35.2		5.99 ± 0.05
	25.5	10	5.12 ± 0.16
		50	6.33 ± 0.07
		100	8.45 ± 0.10
		150	12.0 ± 1.1
1d	15.0	0.1	16.5 ± 0.2
	20.0		17.4 ± 0.3
	25.0		18.4 ± 0.3
	30.1		19.3 ● 0.2
	35.0		20.6 ● 0.2
	25.0	10	18.9 ± 0.5
		50	24.3 ± 0.2
		95	30.5 ± 0.4
		150	45.5 ± 0.6

The extremely low values of $\Delta H^{\ddagger}$ (between 2 and 10 kJ mol^{-1}) and the large negative activation entropies (−121 to −152 J K^{-1} mol^{-1}) are an indication for a multistep mechanism where the first step may involve carbon–nitrogen bond formation between the carbene complex and pyrrolidine through a highly structured transition state.

The $\Delta V^{\ddagger}$ values are significantly negative (ca. −16 cm^3 mol^{-1}) and indicate substantial bond formation during the rate-determining step of the addition process. The determined activation parameters ($\Delta H^{\ddagger}$, $\Delta S^{\ddagger}$, and $\Delta V^{\ddagger}$) for the various complexes are all in good agreement and point at a process in which considerable bond formation occurs in the transition state.

In principle, such a reaction can be classified as a two step process via formation of a zwitterionic intermediate or a one step process involving a transition state either with considerable dipole formation (concerted but nonsychronous one step mechanism) or without significant charge separation (synchronous one step mechanism). It is well-known that both the study of the kinetic isotope effect and the determination of reaction rates and activation parameters in various solvents can be useful to distinguish between different reaction mechanisms. Besides the importance of the kinetic isotope effect, $\Delta V^{\ddagger}$ is in particular a powerful mechanistic parameter, since the values are determined from a slope and not from an extrapolated intercept, as in the case of $\Delta S^{\ddagger}$. Furthermore,

Table V. Rate and Activation Parameters for Reaction 1 in Acetonitrile

complex	$10^{-4}k$ (25 °C), M^{-1} s^{-1}	$\Delta G^{\ddagger}_{298}$, kJ mol^{-1}	$\Delta H^{\ddagger}$, kJ mol^{-1}	$\Delta S^{\ddagger}$, J mol^{-1} k^{-1}	$\Delta V^{\ddagger}$, cm^3 mol^{-1}
1a	2.92 ± 0.04	47.5	2.0 ± 0.2	−152 ± 1	−16.6 ± 0.4
1b	10.3 ± 0.5	44.4	4.4 ± 0.1	−134 ± 1	−16.4 ± 0.3
1c	5.01 ± 0.05	46.2	10.0 ± 0.3	−121 ± 1	−15.0 ± 0.7
1d	18.7 ± 0.3	43.0	5.6 ± 0.3	−125 ± 1	−15.3 ± 0.8

Table VI. Rate Constants as a Function of Temperature and Pressure for the Addition of Pyrrolidine to the Carbene Complex 1c in Different Solvents

solvent	temp, °C	pressure, MPa	$10^{-3}k$,[a] M^{-1} s^{-1}
1,2-dichlorobenzene	16.3	10[b]	7.83 ± 0.05
	25.0		10.5 ± 0.1
	36.5		14.6 ± 0.4
	25.0	10	10.5 ± 0.1
		50	13.4 ± 0.2
		100	19.7 ± 0.2
		150	26.2 ± 1.5
chlorobenzene	16.6	10[b]	5.72 ± 0.03
	25.4		7.7 ± 0.3
	37.6		10.2 ± 0.2
	25.4	10	7.7 ± 0.3
		50	10.5 ± 0.2
		100	15.1 ± 0.3
		150	20.0 ± 0.6
toluene	14.9	10[b]	4.53 ± 0.08
	25.0		6.07 ± 0.16
	36.1		14.7 ± 0.16
	25.0	10	6.2 ± 0.2
		50	7.9 ± 0.2
		100	12.3 ± 0.2
		150	17.2 ± 0.6

[a] Mean value of at least five kinetic runs. [b] The experiments were performed using glass syringes under 10 MPa in the high-pressure stopped-flow instrument because the O-rings in the ambient pressure instrument were not inert against the solvent.

the volume of activation is usually very sensitive toward charge creation/separation in the transition state.[39-43] As pointed out before, $\Delta V^{\ddagger}$ can be considered as a sum of two components as shown in eq 5.

$$\Delta V^{\ddagger}_{obs} = \Delta V^{\ddagger}_{intr} + \Delta V^{\ddagger}_{elec} \quad (5)$$

$\Delta V^{\ddagger}_{intr}$ represents the change in volume due to changes in bond lengths and angles, and $\Delta V^{\ddagger}_{elec}$, the change in volume due to electrostriction, i.e. changes in solvation on forming the transition state.

From the Eyring equation, fundamental thermodynamics, and adaption of the Kirkwood solvation model,[44] eq 6 can be derived where $\mu_{\ddagger}$ and $r_{\ddagger}$ refer to the transition

$$\Delta V^{\ddagger}_{obs} = \Delta V^{\ddagger}_{intr} - N_A\left[\frac{\mu_{\ddagger}^2}{r_{\ddagger}^3} - \sum\frac{\mu_{rgt}^2}{r_{rgt}^3}\right]q_p \quad (6)$$

state, μ_{rgt} and r_{rgt} refer to all reagents taking part in the activation process, and q_p is the pressure derivative of the solvent parameter $q = (\epsilon - 1)/(2\epsilon + 1)$.[40] All of these quantities are accessible with the exception of $\mu_{\ddagger}$, the transition state dipole moment, which can be calculated from the slope of a plot of $\Delta V^{\ddagger}$ versus q_p according to eq 6. $\Delta V^{\ddagger}_{intr}$ can be determined from the intercept of such a plot.

The absence of a primary kinetic isotope effect for the reaction of $(CO)_5WC(OC_2H_5)(C_2C_6H_5)$ with pyrrolidine and *N*-deuteriopyrrolidine (Figure 3) and the small $k_H:k_D$ ratio of 1.2:1, attributed to a secondary isotope effect, support a two step mechanism where the rate-determining step is carbon–nitrogen bond formation followed by a rapid proton transfer from the nitrogen to C(2) of the carbene complex (see (7)). The second-order rate constant for

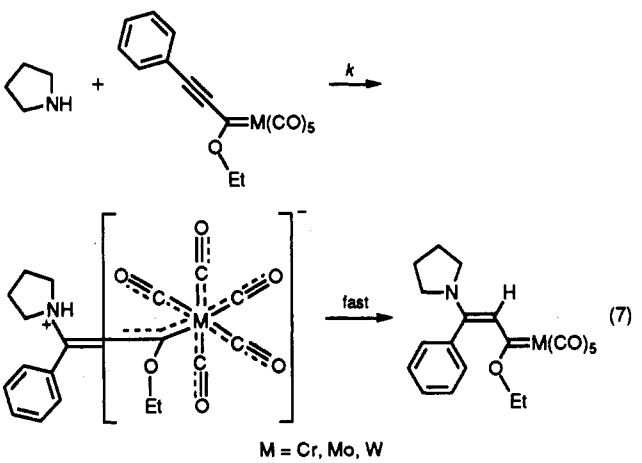

M = Cr, Mo, W

reaction 1 and its dependence on temperature and pressure were studied in five different solvents. The corresponding rate and activation parameters are listed in Tables VI and VII. The selection of the solvents was limited by the experience that the complex reacted with a variety of solvents, i.e. alcohols. They were chosen in such a way that ϵ and q_p vary almost by a factor of 20 (see Table VII). The data in Table VII demonstrate that there is an increase in k with increasing solvent polarity, k(MeCN):k(heptane) = 40:1, which clearly shows that there must be a larger charge separation in the activated complex than in the reactants. A considerably larger solvent effect was reported for the addition of piperidine to methyl propargylate,[45] where the ratio k(MeCN):k(c-C_6H_{12}) = 865:1 was reported.[46] This reaction was also classified as a two step process, where the rate-determining step is, as in eq 7, the formation of a zwitterionic intermediate resulting from carbon–nitrogen bond formation.[47,48] However, the significantly smaller ratio of k(MeCN):k(heptane) for reaction 1 can reasonably be explained in terms of effective charge delocalization on the $(O{\equiv}C)_5M{=}C{-}C{\equiv}C$ moiety (compared to the ester fragment $O{=}C{-}C{\equiv}C$) in the Fischer carbene complex. In organometallic reactions that proceed via a synchronous, one step process, almost no solvent effect (a factor less than 2) was found, as for instance in cycloaddition reactions.[16,49]

The activation parameters $\Delta H^{\ddagger}$ and $\Delta S^{\ddagger}$ also depend to some extent on the solvent, but not in a characteristic way. The volumes of activation, however, show a distinct decrease to more negative values with decreasing dielectric

(39) van Eldik, R.; Asano, T.; le Noble, W. J. *Chem. Rev.* **1989**, *89*, 549.
(40) Isaacs, N. *Liquid Phase High Pressure Chemistry*; John Wiley: Chichester, U.K., 1981.
(41) van Eldik, R., Ed. *Inorganic High Pressure Chemistry, Kinetics and Mechanisms*; Elsevier: Amsterdam, 1986.
(42) Stieger, H.; Kelm, H. *J. Phys. Chem.* **1973**, *77*, 290.
(43) Schmidt, R.; Geis, M.; Kelm, H. *Z. Phys. Chem.* **1974**, *92*, 223.
(44) Kirkwood, J. G. *J. Chem. Phys.* **1934**, *2*, 351.
(45) Giese, B.; Huisgen, R. *Tetrahedron Lett.* **1967**, *20*, 1889.
(46) Reichardt, C. *Solvents and Solvent Effects in Organic Chemistry*; VCH: Weinheim, Germany, 1988.
(47) Huisgen, R.; Giese, B.; Huber, H. *Tetrahedron Lett.* **1967**, *20*, 1883.
(48) Neuenschwander, M.; Bilger, P. *Helv. Chim. Acta* **1973**, *56*, 959.
(49) Halliman, N.; McArdle, P.; Burgess, J.; Guadardo, P. *J. Organomet. Chem.* **1987**, *333*, 77.

Table VII. Rate and Activation Parameters for Reaction 1 (M = W, $R^1 = C_6H_5$, $R^2 = C_2H_5$) in Various Solvents

solvent	ϵ_R[a]	$10^6 q_p$, bar^{-1}	$10^{-3}k$ (25 °C), M^{-1} s^{-1}	$\Delta G^{\ddagger}$, kJ mol^{-1}	$\Delta H^{\ddagger}$, kJ mol^{-1}	$\Delta S^{\ddagger}$, J K^{-1} mol^{-1}	$\Delta V^{\ddagger}$, cm^3 mol^{-1}
acetonitrile	35.9	1.5[b]	50.1 ● 0.2	46.2	10.0 ± 0.3	−121 ● 1	−15.0 ± 0.7
1,2-dichlorobenzene	9.93	5.5[c]	10.4 ± 0.1	50.1	20.6 ± 0.8	−99 ± 3	−16.5 ± 0.6
chlorobenzene	5.62	8.9[b]	7.67 ± 0.10	51.0	18.0 ± 1.7	−111 ± 6	−17.0 ± 0.9
toluene	2.38	14.7[b]	6.20 ± 0.07	51.4	20.6 ± 1.2	−103 ± 4	−18.8 ± 0.8
n-heptane	1.92	25.8[c]	1.28 ± 0.01	55.4	10.6 ± 0.8	−150 ± 3	−21.9 ± 0.7

[a] Reference 46. [b] Reference 43. [c] q_p was calculated from values in ref 40.

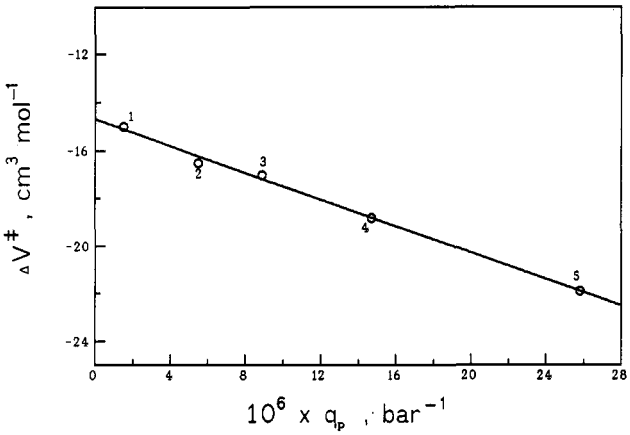

Figure 5. Dependence of the volume of activation at 25 °C for reaction 1 (complex 1c) on the solvent parameter q_p: (1) acetonitrile; (2) 1,2-dichlorobenzene; (3) chlorobenzene; (4) benzene; (5) heptane.

constant of the solvent. In Figure 5, the experimental volumes of activation from Table VII are plotted versus q_p. A fairly good linear relationship results for the five investigated solvents. The intercept ($\Delta V^{\ddagger}_{intr}$) has a value of ca. −14.5 cm^3 mol^{-1}, typical for bimolecular reactions with significant bond formation in the transition state. Values for other organometallic reactions are very similar; viz. $\Delta V^{\ddagger}_{intr}$ for oxidative addition of H_2 and CH_3I to $Ir(Cl)(CO)(PPh_3)_2$ are −18 and −17 cm^3 mol^{-1}, respectively.[42,43] Furthermore, in a theoretical study[50] on a [2 + 2] cycloaddition reaction via a zwitterionic intermediate, −14 cm^3 mol^{-1} was allocated to intrinsic volume changes, which is indeed very close to the value obtained in this study and typical for the formation of a single bond.[39]

According to eq 6, the slope of the straight line in Figure 5 is defined by eq 8. From the available data and the assumptions indicated under eq 8, a dipole moment for the transition state of $\mu_{\ddagger} = 20.3 \pm 0.7$ D was calculated for the addition of pyrrolidine to the carbene complex *1c*. The precision of μ should not be overestimated since the calculation is based on many simplifications. Nevertheless, the result is consistent with the zwitterionic intermediate **6**, since $\mu_{\ddagger}$ is much larger than the sum of the dipole moments of the reaction partners, which would apply if the reaction passed through a cyclic transition state.[43,50,54-56]

Furthermore, $\mu_{\ddagger}$ can be expressed as in (9), where q is the charge and d is the distance of charge separation in

$$\text{slope} = -N_A\left(\frac{\mu_{\ddagger}^2}{r_{\ddagger}^3} - \frac{\mu_{1c}^2}{r_{1c}^3} - \frac{\mu_2^2}{r_2^3}\right) \quad (8)$$

$$\text{slope} = (-2.79 \pm 0.10) \times 10^5 \text{ cm}^3 \text{ mol}^{-1} \text{ bar}$$

$$\mu_{1a}(\text{complex 1a}) \approx \mu_{1c}(\text{complex 1c}) = 5.80 \text{ D}^{21}$$

$$r_{1c} \approx r_{1a} + \Delta(r(\text{Cr}) - r(\text{W})) = (4.70 \pm 0.17) \times 10^{-8} = 4.87 \times 10^{-8} \text{ cm}^{51}$$

$$\mu_2(\text{pyrrolidine}) = 0.80 \text{ D}^{52}$$

$$r_2 = 3.21 \times 10^{-8} \text{ cm}^{53}$$

$$r_{\ddagger} \approx r_{1c} + r_2 = 8.08 \times 10^{-8} \text{ cm}$$

which form it can be related to the relatively small solvent

$$\mu_{\ddagger} = |q|d \quad (9)$$

dependence and small changes in $\Delta V^{\ddagger}_{elec}$. The larger dipole moment of the transition state is presumably caused by a relatively small q value, resulting from an excellent charge delocalization over the $M(CO)_5$ fragment, which results in a small solvent dependence, and a long distance d between the positive and negative charges (from the nitrogen to the $M(CO)_5$ moiety). This charge dilution is also responsible for the small changes in $\Delta V^{\ddagger}_{elec}$ and indicates only a weak interaction between solute and solvent. The larger differences in $\Delta V^{\ddagger}_{elec}$ found for the oxidative addition of CH_3I to the Vaska complex in different solvents,[42] compared to that observed in this study, can be accounted for in terms of a change in the oxidation state from Ir(I) to Ir(III) and considerably less charge delocalization.

Considering all the results of this study, it can be concluded that the addition reactions follow a two step process in which a zwitterionic intermediate **6** is produced in the rate-determining step. The possibility of the pentacarbonyl–carbene fragment to delocalize the charge density demonstrates the advantages of such organometallic reactions over pure organic processes, which results in a significant acceleration of the addition process, as mentioned in the Introduction.

Acknowledgment. The authors gratefully acknowledge financial support from the Deutsche Forschungsgemeinschaft, Fonds der Chemischen Industrie, and Volkswagen-Stiftung.

Supplementary Material Available: Tables of crystal data, atomic coordinates, thermal parameters, and bond distances and angles for compound **3c** (6 pages). Ordering information is given on any current masthead page.

OM920642Y

(50) Fleischmann, F. K.; Kelm, H. *Tetrahedron Lett.* **1973**, *39*, 3773.
(51) Huttner, G.; Lorenz, H. *Chem. Ber.* **1975**, *108*, 1864.
(52) Buckley, P. J.; Costain, C. C.; Parkin, J. E. *J. Chem. Soc., Chem. Commun.* **1968**, 668.
(53) Synoweitz, C.; Schäfer, K. *Chemiker-Kalender*; Springer: Berlin, 1984.
(54) Huisgen, R. *Acc. Chem. Res.* **1977**, *10*, 199.
(55) Steiner, G.; Huisgen, R. *J. Am. Chem. Soc.* **1973**, *95*, 5056.
(56) Huisgen, R.; Feiler, L. A.; Otto, P. *Tetrahedron Lett.* **1968**, *43*, 4485.